ASTRONOMY & ASTROPHYSICS
SUPPLEMENT SERIES

Astron. Astrophys. Suppl. Ser. **129,** 435-443 (1998)

Identification of FeH molecular lines in the spectrum of a sunspot umbra

D.E. Fawzy[1,2], **N.H. Youssef**[1], **and O. Engvold**[3]

[1] Astronomy Department, Faculty of Science, Cairo University, Cairo, Egypt
[2] currently: Institut für Theoretische Astrophysik der Universität Heidelberg, Tiergartenstrasse 15, D-69121 Heidelberg, Germany
[3] Institute of Theoretical Astrophysics, University of Oslo, Blindern, Oslo, Norway

Received August 18; accepted October 7, 1997

Abstract. A high resolution spectrum of a large - sunspot umbra is used for identification of two bands (2−0) and (2−1) of the $^4\Delta-\ ^4\Delta$ system of the FeH molecule, in addition to the previously identified bands (0−0) and (1−0) of the same system. The spectrum was obtained with FTS of the McMath-Pierce Solar Telescope of NSO/NOAO at Kitt Peak.

Key words: molecular data — Sun: atmosphere — Sun: sunspots

1. Introduction

The first identification of lines from the FeH molecule was made in the blue-green part of the solar spectrum by Carroll & McCormack (1972). The molecular origin of a number of weak lines was also demonstrated by the fact that their strengths were enhanced in sunspots (Moore et al. 1966). Klynning & Lindgren (1973) reported that lines of the (0−0) band of FeH extend from 9 896 Å to at least 10 205 Å. Carroll et al. (1976) detected a number of coincidences between laboratory lines of FeH and weak unidentified solar lines, again in the blue and green wavelength region, in addition to the infrared. Wing et al. (1977) confirmed the presence of the (0−0) and (1−0) bands of iron hydride in sunspots and cool stars. They were not be able to identify the infrared FeH bands in the spectrum of the solar disk. Wöhl et al. (1983) measured the strengths of the (0−0) and (1−0) bands of the FeH molecule in the umbral spectrum of a large spot.

It is noticed that the sunspot spectrum from 9 900 Å to 10 100 Å comes close to being a pure FeH spectrum. Since very high resolution solar and laboratory spectra are available, a reinvestigation of the FeH molecule is, therefore, of notable interest.

Send offprint requests to: N.H. Youssef, cu090@frcu.eun.eg

2. Molecular data

Seven infra-red bands of the $^4\Delta-^4\Delta$ system of the FeH molecule were analyzed by Phillips et al. (1987) (The rms of the deviations between observed and calculated lines was 0.01 cm^{-1}). Their wavenumber ranges are listed in Table 1 in order of the wavelength of the heads. The wavelengths and wavenumbers for two additional bands were calculated. Four pairs of R-branches and four pairs of P-branches imply that the infrared system is produced by transitions between two quartet states with Λ-type doubling. The lower energy level in a Λ doubled pair is described as an *a*-level and the higher as a *b*-level. The main branches of the bands due to $^4\Delta_{7/2}-^4\Delta_{7/2}$, $^4\Delta_{5/2}-^4\Delta_{5/2}$, $^4\Delta_{3/2}-^4\Delta_{3/2}$ and $^4\Delta_{1/2}-^4\Delta_{1/2}$ have been studied in the present analysis.

Table 1. I.R. bands of the $^4\Delta-^4\Delta$ system of the FeH molecule

Band	Wavenumber Range (cm^{-1})	Head Wavelength (Å)
(2−0)	12045 – 12846	7786
(1−0)	10343 – 11500	8692
(2−1)	10324 – 11089	9020
(0−0)	8990 – 10102	9896
(1−1)	9191 – 9750	10253
(2−2)*	8750 – 9403	10639
(0−1)	7563 – 8373	11939
(1−2)	7450 – 8069	12389
(0−2)*	6118 – 6697	14927

**Calculated.*

3. Observed solar spectrum

A high resolution spectrum of a large sunspot recorded by Brynildsen et al. (1989) with the Fourier Transform Spectrometer at the McMath telescope of NSO/NOAO at Kitt Peak, is compared with the laboratory FeH spectrum. The present umbral spectrum is from a large sunspot of diameter 29 ± 1 arcsec. The spot is denoted San Fernando 535. The magnetic field strength of this spot umbra is $B_{||} = 3075 \pm 250G$ (Brynildsen et al. 1989). This atlas also gives the corresponding photospheric spectrum from a quiet region very close to the spot.

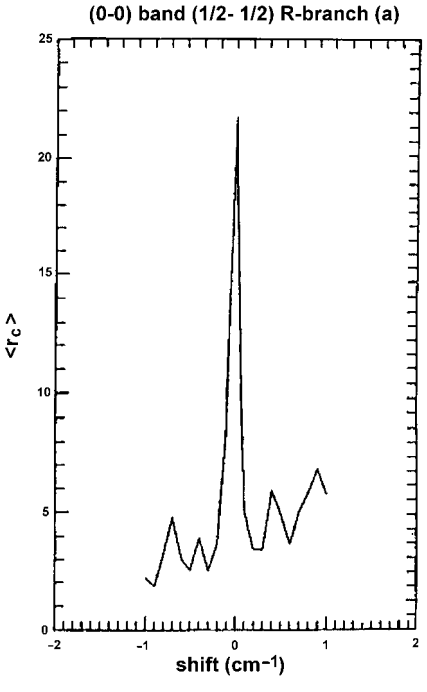

Fig. 1. Example of the coincidence curve for the transition (1/2−1/2) of the R-branch of the (0−0) band

4. FeH Solar identification

The probability of chance coincidence between laboratory and umbral wavenumbers can be tested by means of the Russell-Bowen formula (Engvold et al. 1980). In the method of wavelength coincidence, the procedure of identification is completed as the list of accurate wavelengths for a particular transition of the selected molecule and the stellar spectrum are compared for coincidences (Hansen 1985; Lambert 1988). The method of coincidence assumes an identification of the solar line with a laboratory line if the line is located within 0.05 cm^{-1} of the listed laboratory value. In order to exclude the possibility of identifying a molecular band by chance, the number of coincidences found, should exceed the number of chance coincidences. In addition, the variation of relative line strength with

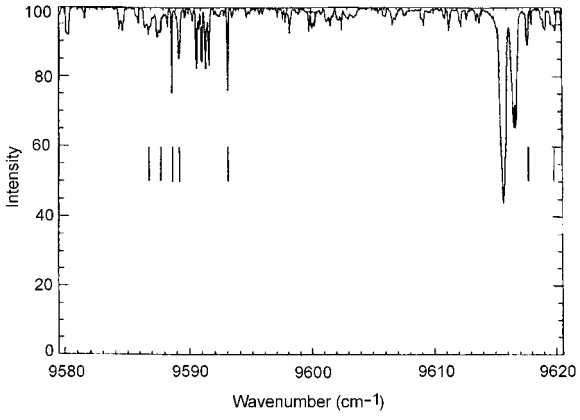

Fig. 2. Part of the umbral spectrum with locations of the FeH lines of the (0−0) band

rotational quantum number J is checked (see Sotirovski 1971). A quantitative measure of the significance of the coincidences is performed by using the following formula (Hansen 1985):

$$\nu_{\mathrm{control}} = \nu_{\mathrm{lab}} + (N \times 0.05 - 1.00) \ \ [\mathrm{cm}^{-1}] \qquad (1)$$

where ν is in cm^{-1} and N represents successively all integer numbers between 0 and 40. An example of the resulting plots of mean residual intensities $< r_{\mathrm{c}} >$ for a given band, versus shift in wavenumber relative to the predicted line positions, is shown in Fig. 1. The presence of a molecular band in the umbral spectrum shows up as a peak above the noise produced by random coincidences. All known FeH bands (Phillips et al. 1987) within the spectral range of the present umbral spectrum were checked with this procedure (Fawzy 1995). A slightly different version of this method was developed and used by Lambert (1988). Figure 1 shows a good example of the coincidence curve for the transition (1/2−1/2) of the lower (a) energy level of the Λ-doublet pair for the R-branch of the FeH (0−0) band. We have searched for all laboratory line positions of the bands (2−0), (1−0), (2−1), (0−0), (1−1), and (2−2) within the available range of the umbral spectrum $\lambda\lambda 5600 - 11600$ Å; $\sigma\sigma = 8000 - 18000$ cm^{-1}). Figure 2 shows a part of the umbral spectrum of the studied sunspot with the locations of FeH lines of the (0−0) band. The laboratory, umbral wavenumbers and their differences $\nu_{\mathrm{lab.}} - \nu_{\mathrm{umb.}}(\mathrm{cm}^{-1})$ are given in Tables 2-5 with the corresponding transitions for the identified bands (0−0), (1−0), (2−0), and (2−1) respectively. The numbers (1), (2), (3), and (4) are used for transitions (7/2−7/2), (5/2−5/2), (3/2−3/2), and (1/2−1/2), respectively, for either the upper (b), or the lower (a) energy level of Λ-doublet pair for both R and P-branches. The differences between laboratory and umbral wavenumbers of the identified lines are less than ± 0.1 cm^{-1}.

5. Conclusions

Using high resolution spectra of a large sunspot umbra obtained with FTS of the McMath-Pierce Solar Telescope of NSO/NOAO at Kitt Peak, we have been able to identify two new bands (2−0) and (2−1) of the $^4\Delta-^4\Delta$ system of FeH molecule. Previously, the two bands (0−0) and (1−0) were identified. The new identification of more than 500 FeH lines in the umbral spectrum confirms that this molecule accounts for the majority of lines in sunspot umbrae in the spectral range $\lambda\lambda 7782-11119$ Å; $\sigma\sigma = 8990-12846$ cm^{-1}. The presence of FeH lines in sunspot umbral spectra offers the possibility to study the higher layers in the umbral atmosphere. The variation of equivalent widths with rotational quantum number reflects the rotational temperature of these layers (Mulchaey 1989; Fawzy et al. 1997, in preparation).

Notes to Tables 2 to 5:

[a] P or R branch. The numbers (1), (2), (3), and (4) are used for transitions (7/2−7/2); (5/2−5/2); (3/2−3/2); and (1/2−1/2) respectively. *a* or *b*: the lower or upper energy level of Λ-doublet pair.
[b] The rotational quantum numbers.
[c] Laboratory wavenumbers taken from Phillips et al. (1987).
[d] Line transitions in the umbral spectrum.
[e] The numbers in the parentheses represent doubtful coincidences where $\nu_{\rm lab.}-\nu_{\rm umb.} > 0.1$ cm^{-1}. Most of these lines are not included in the determination of the rotational temperature.

Acknowledgements. Fawzy and Youssef are indebted to the German GTZ for offering Astronomy Department a SunSparc station. Fawzy is indebted to Mr. Amer of Cairo University for his kind help in using the IDL package. Engvold thanks the Astronomy Department, Faculty of Science, Cairo University, for the warm hospitality shown him during his visit.

References

Brynildsen N., Engvold O., Hansteen V., Brault J.W., 1989, An Umbral Spectrum of a Large Sunspot ($\sigma\sigma$ 8000 − 18000 cm^{-1})
Carroll P.K., McCormack P., 1972, ApJ 177, L33
Carroll P.K., McCormack P., O'Connor S., 1976, ApJ 208, 903
Engvold O., Wöhl H., Brault J.W., 1980, A&AS 42, 209
Fawzy D.E., 1995, M. Sci.-Thesis, Cairo University
Hansen K., 1985, M. Sci.-Thesis, University of Oslo
Klynning L., Lindgren B., 1973, Univ. Stockholm Inst Phys. USIP, Rept. 73-20
Lambert D.L., 1988, PASP 100, 1202
McCormack P., O'Connor S., 1976, A&AS 26, 373
Moore C.E., Minnaert M.C.J., Houtgast J., 1966, Second Revised Rowland's Preliminary Tables of Solar Spectrum Wavelenghts, N.B.S. Monograph, p. 61
Mulchaey J.S., 1989, PASP 101, 211
Phillips J.G., Davis S.P., Lindgren B., Balfour W.J., 1987, APJS 65, 721
Sotirovski P., 1971, A&A 14, 319
Wing R.F., Cohen J., Brault J.W., 1977, AJ 216, 659
Wöhl H., Engvold O., Brault J.W., 1983, Institute of Theoretical Astrophysics, Univ. Oslo, Report No. 56

Table 2. FeH lines of the (0−0) band identified in the umbral spectrum

Transition[a]	$J^{(b)}$	$\nu^{(c)}_{\rm lab.}$	$\nu^{(d)}_{\rm umb.}$	$\nu_{\rm lab.}-\nu^{(e)}_{\rm umb.}$
P(3)a	24.5	9210.218	9210.300	−.082
P(4)b	21.5	9218.716	9218.777	−.062
P(2)a	27.5	9239.031	9239.199	(−.168)
P(3)a	23.5	9262.826	9262.725	(.102)
P(4)b	20.5	9270.139	9270.095	.044
P(2)a	26.5	9288.559	9288.540	.019
P(2)b	25.5	9291.756	9291.753	.003
P(3)a	22.5	9313.948	9313.989	−.041
P(2)a	25.5	9336.237	9336.280	−.043
P(2)b	24.5	9338.715	9338.858	(−.144)
P(3)a	21.5	9363.582	9363.421	(.161)
P(4)b	18.5	9369.574	9369.557	.018
P(2)a	24.5	9382.119	9382.063	.056
P(2)b	23.5	9384.058	9384.188	(−.131)
P(1)b	26.5	9398.729	9398.690	.038
P(3)a	20.5	9411.757	9411.651	(.105)
P(4)a	17.5	9415.849	9415.809	.040
P(4)b	17.5	9417.308	9417.279	.028
P(2)a	23.5	9426.169	9426.174	−.005
P(2)b	22.5	9427.723	9427.861	(−.139)
P(1)a	26.5	9430.942	9430.930	.013
P(3)a	19.5	9458.412	9458.433	−.021
P(4)a	16.5	9460.237	9460.248	−.011
P(4)b	16.5	9463.581	9463.552	.029
P(1)a	25.5	9467.654	9467.636	.019
P(2)a	22.5	9468.480	9468.435	.046
P(2)b	21.5	9470.331	9470.468	(−.137)
P(4)a	15.5	9500.902	9500.928	−.025
P(3)b	18.5	9502.009	9502.071	−.063
P(3)a	18.5	9503.537	9503.560	−.022
P(4)b	15.5	9508.359	9508.334	.025
P(2)a	21.5	9508.996	9508.987	.009
P(2)b	20.5	9510.891	9511.002	(−.111)
P(1)b	23.5	9516.651	9516.647	.004
P(1)a	23.5	9538.191	9538.215	−.023
P(3)b	17.5	9541.717	9541.772	−.056
P(4)a	14.5	9546.291	9546.293	−.002

Table 2. continued

Transition[(a)]	$J^{(b)}$	$\nu^{(c)}_{\rm lab.}$	$\nu^{(d)}_{\rm umb.}$	$\nu_{\rm lab.} - \nu^{(e)}_{\rm umb.}$
P(3)a	17.5	9547.176	9547.146	.029
P(2)a	20.5	9547.618	9547.690	−.072
P(2)b	19.5	9550.665	9550.722	−.057
P(4)b	14.5	9551.616	9551.611	.005
P(1)b	22.5	9552.429	9552.520	−.091
P(1)a	24.5	9570.933	9570.907	.025
P(3)b	16.5	9580.204	9580.274	−.070
P(1)b	21.5	9586.726	9586.791	−.065
P(2)b	18.5	9587.609	9587.734	(−.125)
P(4)a	13.5	9588.665	9588.660	.005
P(3)a	16.5	9589.267	9589.224	.043
P(4)b	13.5	9593.152	9593.126	.026
P(3)b	15.5	9617.703	9617.725	−.021
P(2)a	18.5	9619.823	9619.830	−.007
P(1)b	20.5	9620.731	9620.848	(−.116)
P(2)b	15.5	9623.748	9623.860	(−.112)
P(3)a	15.5	9629.797	9629.796	.001
P(4)a	12.5	9629.797	9629.796	.001
P(4)b	12.5	9633.252	9633.245	.007
P(1)b	19.5	9642.151	9642.249	−.098
P(2)a	17.5	9653.210	9653.230	−.021
P(3)b	14.5	9654.317	9654.356	−.039
P(2)b	16.5	9658.389	9658.332	.057
P(1)a	19.5	9658.608	9658.495	(.113)
P(3)a	14.5	9668.700	9668.660	.040
P(4)a	11.5	9669.675	9669.659	.016
P(4)b	11.5	9672.182	9672.164	.018
P(1)a	18.5	9684.318	9684.274	.044
P(2)a	16.5	9685.080	9684.982	.098
P(3)b	13.5	9689.876	9689.883	−.007
P(2)b	15.5	9691.349	9691.462	(−.113)
P(1)b	17.5	9698.180	9698.143	.037
P(4)b	8.5	9704.680	9704.460	(.220)
P(3)a	13.5	9706.021	9706.021	.000
P(4)a	10.5	9708.197	9708.199	−.002
P(1)a	17.5	9708.269	9708.199	.069
P(2)a	15.5	9715.224	9715.260	−.036
P(2)b	14.5	9723.004	9723.102	−.098
P(3)b	12.5	9724.490	9724.500	−.010
P(1)a	16.5	9730.704	9730.799	−.095
P(4)b	9.5	9741.188	9741.164	.024
P(3)a	12.5	9741.542	9741.509	.033
P(2)a	6.5	9743.776	9743.777	−.001
P(4)a	9.5	9745.242	9745.229	.014
P(1)a	15.5	9751.224	9751.274	−.051

Table 2. continued

Transition[(a)]	$J^{(b)}$	$\nu^{(c)}_{\rm lab.}$	$\nu^{(d)}_{\rm umb.}$	$\nu_{\rm lab.} - \nu^{(e)}_{\rm umb.}$
R(4)b	20.5	9752.424	9752.363	.061
P(2)b	13.5	9753.138	9753.253	(−.115)
R(3)a	24.5	9756.229	9756.303	−.074
P(3)b	11.5	9758.045	9758.027	.018
P(2)a	13.5	9770.756	9770.755	.001
P(4)b	8.5	9774.523	9774.530	−.007
P(3)a	11.5	9775.430	9775.438	−.009
P(4)a	8.5	9780.628	9780.629	−.001
P(2)b	4.5	9781.798	9781.863	−.065
R(4)b	9.5	9782.930	9782.971	−.041
P(l)b	13.5	9783.752	9783.788	−.036
P(1)a	13.5	9787.518	9787.636	(−.118)
R(3)a	23.5	9790.437	9790.359	.077
P(3)b	10.5	9790.545	9790.559	−.014
P(2)a	12.5	9796.365	9796.494	(−.129)
P(l)b	12.5	9800.601	9800.797	(−.196)
P(1)a	12.5	9803.344	9803.338	.006
P(4)b	7.5	9805.940	9805.952	−.012
P(3)a	10.5	9807.560	9807.586	−.026
P(2)b	11.5	9809.012	9809.092	−.080
R(4)b	18.5	9811.783	9811.815	−.032
P(4)a	7.5	9814.166	9814.175	−.009
P(1)b	11.5	9815.796	9815.827	−.031
P(1)a	11.5	9817.713	9817.823	(−.110)
P(2)a	11.5	9820.603	9820.691	−.089
P(3)b	9.5	9821.956	9821.944	.012
R(3)a	22.5	9822.738	9822.652	.086
P(1)a	10.5	9830.717	9830.856	(−.140)
P(2)b	10.5	9834.795	9834.851	−.056
P(4)b	6.5	9835.589	9835.576	.013
P(3)a	9.5	9837.884	9837.863	.021
R(4)b	17.5	9838.889	9838.880	.009
P(l)b	9.5	9841.668	9841.823	(−.155)
P(1)a	9.5	9842.462	9842.622	(−.160)
P(2)a	10.5	9843.596	9843.693	−.098
P(4)a	6.5	9845.628	9845.617	.011
R(2)b	25.5	9846.259	9846.071	(.188)
P(3)b	8.5	9852.170	9852.152	.018
P(1)b	8.5	9852.624	9852.751	(−.127)
P(1)a	8.5	9853.079	9853.096	−.017
R(3)a	21.5	9853.172	9853.096	.076
P(2)b	9.5	9859.204	9859.231	−.027
R(4)a	16.5	9860.970	9860.956	.014
P(1)b	7.5	9862.493	9862.590	−.097
P(1)a	7.5	9862.728	9862.844	(−.116)

Table 2. continued

Transition[(a)]	$J^{(b)}$	$\nu^{(c)}_{\rm lab.}$	$\nu^{(d)}_{\rm umb.}$	$\nu_{\rm lab.} - \nu^{(e)}_{\rm umb.}$
R(4)b	16.5	9864.178	9864.133	.045
P(3)a	8.5	9866.431	9866.420	.011
P(1)a	6.5	9871.592	9871.575	.017
P(4)a	5.5	9874.770	9874.770	.000
R(2)b	24.5	9874.964	9874.770	(.194)
P(3)b	7.5	9881.113	9881.105	.008
R(3)a	20.5	9881.723	9881.668	.055
P(2)b	8.5	9882.297	9883.029	(−.732)
R(4)a	15.5	9883.426	9883.374	.052
P(2)a	8.5	9886.308	9886.388	−.080
R(4)b	15.5	9887.588	9887.567	.021
R(2)a	25.5	9890.362	9890.345	.018
P(3)a	7.5	9893.175	9893.141	.034
R(2)b	23.5	9901.621	9901.617	.004
P(2)b	7.5	9904.216	9904.249	−.033
R(4)a	14.5	9904.964	9904.939	.024
P(2)a	7.5	9906.241	9906.282	−.041
R(3)a	19.5	9908.407	9908.442	−.035
P(3)b	6.5	9908.610	9908.569	.041
R(4)b	14.5	9909.074	9909.042	.032
R(2)a	24.5	9918.159	9918.136	.023
P(3)a	6.5	9918.159	9918.136	.023
P(2)a	17.5	9925.339	9925.399	−.061
R(2)b	22.5	9926.507	9926.634	(−.127)
R(4)b	13.5	9928.611	9928.612	−.001
R(3)b	18.5	9933.103	9933.169	−.066
R(3)a	18.5	9933.260	9933.169	.091
R(4)a	12.5	9942.821	9942.808	.014
R(2)a	5.5	9943.658	9943.697	−.039
R(4)b	7.5	9946.214	9946.202	.012
R(2)b	21.5	9949.437	9949.470	−.033
R(3)a	17.5	9956.230	9956.186	.045
R(4)a	11.5	9960.192	9960.180	.013
R(4)b	11.5	9961.693	9961.687	.007
R(2)b	20.5	9970.354	9970.326	.027
R(3)b	16.5	9970.567	9970.326	(.241)
R(4)a	10.5	9975.777	9975.754	.023
R(3)a	16.5	9977.310	9977.261	.049
R(3)b	15.5	9986.372	9986.409	−.037
R(1)b	9.5	9987.588	9987.553	.035
R(4)b	25.5	9987.588	9987.553	.035
R(2)a	21.5	9988.210	9988.370	(−.160)
R(4)a	9.5	9989.560	9989.532	.027
R(4)b	8.5	9993.085	9993.090	−.005

Table 2. continued

Transition[(a)]	$J^{(b)}$	$\nu^{(c)}_{\rm lab.}$	$\nu^{(d)}_{\rm umb.}$	$\nu_{\rm lab.} - \nu^{(e)}_{\rm umb.}$
R(3)a	15.5	9996.551	9996.502	.049
R(3)b	14.5	10000.781	10000.810	−.028
R(4)a	8.5	10001.412	10001.410	−.002
R(4)b	7.5	10002.339	10002.330	.009
R(2)b	18.5	10007.130	10007.180	−.050
R(2)a	20.5	10007.321	10007.450	(−.129)
R(4)b	6.5	10008.203	10008.200	.003
R(l)b	24.5	10008.332	10008.320	.012
R(4)a	7.5	10011.149	10011.150	−.001
R(4)a	6.5	10018.571	10018.560	.012
R(2)b	17.5	10023.288	10023.290	−.002
R(2)a	19.5	10024.326	10024.420	−.094
R(3)b	12.5	10026.269	10026.250	.019
R(1)b	17.5	10027.032	10027.110	−.078
R(3)a	13.5	10029.268	10029.250	.018
R(1)a	24.5	10034.950	10035.060	(−.109)
R(2)b	16.5	10036.360	10036.290	.070
R(3)b	11.5	10037.273	10037.270	.004
R(2)a	18.5	10039.163	10039.120	.043
R(1)a	7.5	10040.773	10040.910	(−.137)
R(3)a	12.5	10042.859	10042.830	.029
R(3)b	10.5	10047.148	10047.130	.019
R(2)b	15.5	10048.397	10048.400	−.003
R(1)a	23.5	10049.375	10049.260	(.115)
R(2)a	17.5	10052.131	10052.270	(−.139)
R(1)a	8.5	10053.128	10053.110	.018
R(3)a	11.5	10054.469	10054.490	−.021
R(3)b	9.5	10055.747	10055.720	.027
R(2)b	14.5	10058.716	10058.710	.006
R(1)a	22.5	10062.848	10063.000	(−.152)
R(2)a	16.5	10063.020	10063.000	.020
R(3)b	8.5	10063.020	10063.000	.020
R(3)a	10.5	10063.983	10063.960	.023
R(1)a	9.5	10064.418	10064.390	.028
R(2)b	13.5	10067.162	10067.260	−.098
R(3)b	7.5	10068.880	10068.860	.020
R(1)b	20.5	10070.254	10070.260	−.006
R(3)a	9.5	10071.606	10071.540	.066
R(2)a	15.5	10072.077	10072.020	.058
R(1)b	10.5	10073.166	10073.120	.046
R(3)b	6.5	10073.166	10073.120	.046
R(2)b	12.5	10074.135	10074.230	−.096
R(1)a	10.5	10074.476	10074.430	.046
R(3)a	3.5	10077.248	10077.230	.018

Table 2. continued

Transition[(a)]	$J^{(b)}$	$\nu^{(c)}_{\rm lab.}$	$\nu^{(d)}_{\rm umb.}$	$\nu_{\rm lab.} - \nu^{(e)}_{\rm umb.}$
R(2)a	14.5	10079.426	10097.330	.096
R(2)b	11.5	10079.426	10079.330	.096
R(1)b	19.5	10080.826	10080.750	.076
R(3)a	7.5	10080.923	10080.950	−.027
R(3)a	6.5	10082.680	10082.640	.040
R(1)a	11.5	10083.153	10083.240	−.087
R(2)b	10.5	10083.153	10083.240	−.087
R(1)a	20.5	10083.917	10084.000	−.083
R(2)a	6.5	10084.272	10084.220	.053
R(2)a	13.5	10084.910	10084.950	−.040
R(2)b	7.5	10085.328	10085.340	−.012
R(2)a	7.5	10087.719	10087.810	−.091
R(1)b	17.5	10088.036	10088.090	−.054
R(2)a	12.5	10088.782	10088.700	.082
R(2)a	8.5	10090.231	10090.300	−.068
R(1)a	12.5	10090.335	10090.300	.035
R(1)a	19.5	10090.954	10090.970	−.016
R(2)a	11.5	10091.080	10090.970	(.110)
R(2)a	9.5	10091.715	10091.840	(−.125)
R(1)b	13.5	10092.014	10092.030	−.016
R(2)a	10.5	10092.014	10092.030	−.016
R(1)b	16.5	10093.116	10093.100	.016
R(1)b	14.5	10094.571	10094.570	.001
R(1)a	13.5	10095.918	10096.050	(−.132)
R(1)a	18.5	10096.951	10097.090	(−.139)
R(1)a	14.5	10099.866	10100.070	(−.204)
R(1)a	17.5	10100.506	10100.570	−.064
R(1)a	15.5	10101.807	10101.990	(−.184)
R(1)a	16.5	10102.113	10102.190	−.077

Table 3. FeH lines of the (1−0) band identified in the umbral spectrum

Transition[(a)]	$J^{(b)}$	$\nu^{(c)}_{\rm lab.}$	$\nu^{(d)}_{\rm umb.}$	$\nu_{\rm lab.} - \nu^{(e)}_{\rm umb.}$
P(4)b	18.5	10692.148	10692.310	(−.162)
P(1)b	25.5	10743.190	10743.290	−.100
P(4)b	17.5	10749.010	10749.030	−.020
P(4)a	17.5	10772.090	10772.140	−.050
P(3)b	19.5	10780.719	10780.830	(−.111)
P(1)b	24.5	10792.024	10791.940	.084
P(4)b	13.5	10804.116	10804.170	−.054
P(1)a	24.5	10807.039	10807.270	(−.231)
P(4)a	16.5	10824.148	10824.180	−.032
P(1)b	23.5	10839.981	10839.960	.021
P(3)b	18.5	10841.506	10841.580	−.074
P(1)a	23.5	10852.959	10853.070	(−.111)
P(4)b	15.5	10857.738	10857.430	(.308)
P(4)a	15.5	10875.626	10875.900	(−.274)
P(3)b	17.5	10894.334	10894.420	−.086
P(1)a	21.5	10896.123	10896.380	(−.257)
P(4)b	14.5	10910.096	10910.060	.036
P(4)a	14.5	10925.737	10925.810	−.073
P(1)b	21.5	10927.096	10927.170	−.074
P(1)a	21.5	10936.795	10936.830	−.035
P(3)b	16.5	10944.613	10944.760	(−.147)
P(4)b	13.5	10960.746	10960.830	−.084
P(1)b	20.5	10966.338	10966.250	.088
P(4)a	13.5	10974.420	10974.400	.020
P(1)a	20.5	10975.122	10975.220	−.098
P(3)b	17.5	10991.747	10991.640	(.107)
P(4)b	19.5	11008.866	11009.260	−.394
P(4)a	12.5	11021.520	11021.490	.030
P(3)b	14.5	11035.918	11035.960	−.042
P(1)b	10.5	11043.599	11043.550	.049
P(1)a	18.5	11044.120	11044.270	(−.150)
P(4)b	11.5	11055.939	11055.950	−.011
P(4)a	11.5	11066.940	11066.920	.020
P(1)b	8.5	11073.884	11073.750	(.134)
P(3)b	13.5	11077.737	11077.830	−.093
P(4)b	10.5	11100.077	11100.050	.027
P(1)a	16.5	11107.263	11107.150	(.113)
P(4)a	10.5	11110.465	11110.440	.025
P(1)a	12.5	11200.425	11200.430	−.005
R(3)a	20.5	11200.724	11200.770	.046
P(4)b	7.5	11216.182	11216.180	.002
P(1)b	11.5	11217.202	11217.110	.092
P(1)a	15.5	11219.298	11219.490	(−.192)
R(4)b	11.5	11219.298	11219.490	(−.192)

Table 3. continued

Transition[(a)]	$J^{(b)}$	$\nu^{(c)}_{\rm lab.}$	$\nu^{(d)}_{\rm umb.}$	$\nu_{\rm lab.} - \nu^{(e)}_{\rm umb.}$
P(4)a	7.5	11228.734	11228.740	−.006
P(3)b	9.5	11231.061	11231.040	.021
P(1)b	10.5	11235.035	11235.000	.035
R(3)a	19.5	11235.403	11235.370	.033
P(1)a	10.5	11236.392	11236.650	(−.258)
R(1)b	26.5	11237.924	11237.910	.014
R(4)a	15.5	11239.665	11239.690	−.025
R(4)b	14.5	11249.586	11249.570	.016
P(4)b	6.5	11249.845	11249.800	.045
P(1)b	9.5	11250.999	11250.930	.069
P(1)a	9.5	11251.816	11251.730	.086
P(4)a	6.5	11263.302	11263.210	.092
P(1)b	8.5	11265.246	11265.370	(−.124)
P(3)b	8.5	11265.396	11265.370	.026
R(2)b	21.5	11265.808	11265.810	−.002
P(1)a	8.5	11265.808	11265.810	−.002
R(1)b	25.5	11269.103	11269.150	−.047
R(3)a	18.5	11271.470	11271.490	−.020
R(3)b	17.5	11272.963	11272.920	.043
R(4)b	13.5	11277.994	11277.920	.074
P(1)b	7.5	11277.994	11278.080	−.086
P(1)a	7.5	11278.236	11278.320	−.084
P(1)b	6.5	11289.473	11289.480	−.007
P(1)a	6.5	11289.579	11289.680	(−.101)
R(4)a	13.5	11296.590	11296.580	.010
R(2)b	20.5	11296.590	11296.580	.010
P(3)b	7.5	11297.871	11297.870	.001
R(1)b	24.5	11300.877	11300.970	−.093
R(3)a	17.5	11303.363	11303.400	−.037
R(4)b	12.5	11304.688	11304.660	.028
R(3)b	4.5	11310.076	11310.080	−.004
R(4)a	12.5	11322.268	11322.250	.018
R(2)b	19.5	11324.883	11324.900	−.017
P(3)b	6.5	11328.408	11328.390	.018
R(4)b	11.5	11329.337	11329.330	.007
R(1)b	23.5	11330.365	11330.460	−.095
R(3)a	16.5	11332.890	11332.870	.020
R(3)b	15.5	11338.985	11338.970	.015
R(4)a	11.5	11345.949	11345.920	.029
R(4)b	10.5	11351.006	11351.000	.006
R(1)b	22.5	11356.420	11356.390	.030
R(3)a	15.5	11360.098	11360.060	.038
R(3)b	14.5	11365.188	11365.180	.008
R(4)a	10.5	11367.492	11367.470	.022
R(4)b	9.5	11371.351	11371.330	.021

Table 3. continued

Transition[(a)]	$J^{(b)}$	$\nu^{(c)}_{\rm lab.}$	$\nu^{(d)}_{\rm umb.}$	$\nu_{\rm lab.} - \nu^{(e)}_{\rm umb.}$
R(2)b	17.5	11375.258	11375.370	(−.112)
R(1)b	21.5	11381.243	11381.390	(−.147)
R(3)a	14.5	11384.871	11384.850	.021
R(4)a	9.5	11386.823	11386.780	.043
R(3)b	13.5	11388.083	11388.070	.013
R(4)b	8.5	11388.482	11388.430	.052
R(1)a	21.5	11389.150	11389.200	−.050
R(2)b	16.5	11396.974	11396.940	.034
R(1)b	20.5	11401.900	11401.940	−.040
R(4)b	7.5	11402.664	11402.630	.034
R(4)a	8.5	11403.671	11403.780	(−.109)
R(3)a	13.5	11407.275	11407.280	−.005
R(3)b	12.5	11407.872	11407.840	.032
R(1)a	20.5	11409.109	11409.110	-.001
R(4)b	6.5	11413.691	11413.650	.041
R(2)b	15.5	11416.626	11416.700	−.074
R(4)a	7.5	11418.010	11417.970	.040
R(1)b	19.5	11421.195	11421.270	−.075
R(3)b	11.5	11425.136	11425.100	.036
R(1)a	19.5	11426.321	11426.190	(.131)
R(3)a	12.5	11427.283	11427.220	.063
R(4)a	6.5	11429.532	11429.490	.042
R(2)b	14.5	11433.732	11433.780	−.048
R(1)b	18.5	11436.445	11436.610	(−.165)
R(1)a	6.5	11440.284	11440.210	.074
R(3)b	10.5	11440.495	11440.480	.015
R(1)a	18.5	11440.935	11440.900	.035
R(3)a	11.5	11444.828	11444.780	.048
R(2)b	13.5	11449.102	11449.100	.002
R(1)b	2.5	11449.872	11449.810	.062
R(1)a	7.5	11450.131	11450.030	(.101)
R(1)b	17.5	11450.131	11450.030	(.101)
R(1)a	17.5	11450.757	11450.810	−.053
R(3)b	9.5	11455.494	11455.460	.034
R(1)b	8.5	11458.255	11458.090	(.165)
R(1)a	8.5	11458.805	11458.850	−.045
R(3)a	10.5	11459.868	11459.810	.058
R(1)a	16.5	11461.916	11461.840	.076
R(2)b	12.5	11462.266	11462.150	(.116)
R(1)b	16.5	11465.015	11465.050	−.035
R(1)a	9.5	11466.004	11465.940	.064
R(3)b	8.5	11467.963	11467.920	.043
R(1)b	13.5	11468.484	11468.520	−.036
R(1)a	15.5	11469.634	11469.760	(−.126)
R(1)b	10.5	11469.867	11469.990	(−.123)

Table 3. continued

Transition[a]	$J^{(b)}$	$\nu^{(c)}_{\rm lab.}$	$\nu^{(d)}_{\rm umb.}$	$\nu_{\rm lab.} - \nu^{(e)}_{\rm umb.}$
R(1)b	15.5	11470.725	11470.860	(−.135)
R(1)a	10.5	11471.557	11471.590	−.033
R(3)a	9.5	11472.422	11472.390	.032
R(1)b	12.5	11472.422	11472.390	.032
R(1)b	11.5	11472.510	11472.590	−.080
R(2)b	11.5	11473.384	11473.480	−.096
R(1)a	11.5	11475.314	11475.370	−.056
R(1)a	14.5	11476.427	11476.200	(.227)
R(1)a	3.5	11477.184	11477.220	−.036
R(1)a	13.5	11477.354	11477.510	(−.156)
R(3)b	7.5	11477.984	11477.940	.044
R(1)b	11.5	11479.555	11479.580	−.025
R(2)b	10.5	11482.306	11482.340	−.034
R(3)a	8.5	11482.388	11482.340	.048
R(3)b	6.5	11486.375	11486.330	.045
R(3)a	7.5	11488.155	11488.190	−.035
R(2)b	5.5	11489.388	11489.400	−.012
R(2)b	8.5	11494.525	11494.450	.075
R(2)b	7.5	11497.812	11497.750	.062
R(2)b	9.5	11499.212	11499.170	.042

Table 4. FeH lines of the (2−0) band identified in the umbral spectrum

Transition[a]	$J^{(b)}$	$\nu^{(c)}_{\rm lab.}$	$\nu^{(d)}_{\rm umb.}$	$\nu_{\rm lab.} - \nu^{(e)}_{\rm umb.}$
P(1)a	18.5	12338.419	12338.250	(.169)
P(1)a	17.5	12375.248	12375.340	−.092
P(1)a	16.5	12407.106	12407.120	−.014
R(4)a	17.5	12431.650	12431.720	−.070
R(4)a	16.5	12473.458	12473.490	−.032
P(1)a	13.5	12489.636	12489.760	(−.124)
R(4)a	15.5	12513.496	12513.280	(.216)
P(1)a	12.5	12515.455	12515.530	−.075
P(4)b	8.5	12519.067	12519.050	.017
R(4)b	15.5	12519.067	12519.050	.017
P(1)a	11.5	12538.354	12538.410	−.056
R(4)a	14.5	12551.361	12551.330	.031
R(4)b	14.5	12556.947	12557.040	−.093
R(3)b	17.5	12559.792	12559.660	(.132)
P(1)a	10.5	12560.266	12560.190	.076
P(1)a	9.5	12579.871	12579.880	−.009
R(4)a	13.5	12586.960	12586.920	.040
R(4)b	13.5	12591.847	12591.790	.057
R(3)b	16.5	12595.617	12595.640	−.023
P(1)a	8.5	12597.512	12597.540	−.028
P(1)a	7.5	12611.990	12612.130	(−.140)
R(1)b	21.5	12617.834	12617.880	−.046
R(4)a	12.5	12620.188	12620.170	.018
P(1)a	6.5	12627.011	12626.930	.081
R(4)b	12.5	12627.652	12627.660	−.008
R(3)b	15.5	12629.785	12629.770	.015
R(2)b	17.5	12643.399	12643.350	.049
R(1)b	20.5	12646.468	12646.450	.018
R(4)a	11.5	12650.909	12650.860	.049
R(4)b	11.5	12652.747	12652.710	.037
R(3)b	14.5	12660.443	12660.500	−.057
R(2)b	16.5	12673.946	12674.020	−.074
R(1)b	19.5	12674.268	12674.240	.028
R(4)b	10.5	12678.676	12678.630	.046
R(4)a	10.5	12679.080	12679.050	.030
R(3)b	13.5	12689.698	12689.730	−.032
R(4)b	9.5	12701.590	12701.560	.030
R(2)b	15.5	12701.871	12701.820	.051
R(4)a	9.5	12705.031	12705.010	.021
R(3)b	12.5	12714.435	12714.490	−.055
R(1)b	17.5	12720.732	12720.830	−.098
R(4)b	8.5	12721.623	12721.610	.013
R(2)b	14.5	12726.966	12726.870	.096

Table 4. continued

Transition[(a)]	$J^{(b)}$	$\nu^{(c)}_{\rm lab.}$	$\nu^{(d)}_{\rm umb.}$	$\nu_{\rm lab.} - \nu^{(e)}_{\rm umb.}$
R(4)a	8.5	12726.966	12726.870	.096
R(4)b	7.5	12738.670	12738.670	.000
R(1)b	16.5	12738.904	12738.830	.074
R(4)a	7.5	12746.392	12746.450	−.058
R(2)b	13.5	12749.427	12749.410	.017
R(4)b	6.5	12752.787	12752.660	(.127)
R(1)b	15.5	12754.731	12754.750	−.019
R(4)a	6.5	12760.329	12760.420	−.091
R(3)b	10.5	12761.864	12761.850	.014
R(1)b	14.5	12767.743	12767.860	(−.117)
R(2)b	12.5	12769.368	12769.350	.018
R(1)b	6.5	12771.778	12771.620	(.158)
R(1)b	7.5	12777.275	12777.280	−.005
R(1)b	8.5	12781.060	12781.030	.030
R(3)b	9.5	12781.453	12781.470	−.017
R(1)b	9.5	12781.729	12781.780	−.051
R(1)b	11.5	12783.854	12783.830	.024
R(1)b	12.5	12786.305	12786.350	−.045
R(2)b	11.5	12786.382	12786.350	.032
R(3)b	8.5	12799.648	12799.600	.048
R(2)b	10.5	12801.109	12801.080	.029
R(2)b	9.5	12813.443	12813.500	−.057
R(3)b	7.5	12815.172	12815.150	.022
R(2)b	8.5	12823.674	12823.660	.014
R(3)a	8.5	12828.285	12828.250	.035
R(2)b	7.5	12830.757	12830.650	(.107)
R(2)b	6.5	12836.191	12836.200	−.009

Table 5. FeH lines of (2−1) band identified in the umbral spectrum

Transition[(a)]	$J^{(b)}$	$\nu^{(c)}_{\rm lab.}$	$\nu^{(d)}_{\rm umb.}$	$\nu_{\rm lab.} - \nu^{(e)}_{\rm umb.}$
P(4)a	17.5	10324.103	10324.220	(−.117)
P(4)b	17.5	10357.595	10357.780	(−.185)
P(4)b	16.5	10412.930	10412.900	.030
P(3)a	18.5	10441.146	10441.220	−.074
P(4)b	15.5	10466.112	10466.100	.012
P(3)a	16.5	10543.497	10543.490	.007
P(4)a	13.5	10564.382	10564.370	.012
P(4)a	12.5	10610.671	10610.670	.001
P(4)b	12.5	10612.856	10612.760	.096
P(3)a	14.5	10640.774	10640.750	.024
P(1)b	14.5	10735.200	10735.170	.030

Table 5. continued

Transition[(a)]	$J^{(b)}$	$\nu^{(c)}_{\rm lab.}$	$\nu^{(d)}_{\rm umb.}$	$\nu_{\rm lab.} - \nu^{(e)}_{\rm umb.}$
P(4)a	9.5	10743.033	10743.020	.013
P(1)b	12.5	10761.710	10761.870	(−.160)
P(3)a	11.5	10772.291	10772.140	(.151)
P(4)b	8.5	10776.377	10776.340	.037
P(4)a	19.5	10780.719	10780.830	(−.111)
P(1)b	11.5	10787.535	10787.570	−.035
P(1)b	10.5	10808.608	10808.590	.018
P(4)b	7.5	10811.548	10811.540	.008
R(4)b	15.5	10813.575	10813.510	.065
P(4)a	7.5	10815.165	10815.170	−.005
P(3)a	10.5	10819.773	10819.670	(.103)
P(1)b	9.5	10826.797	10826.720	.077
P(1)b	8.5	10843.363	10843.450	−.087
R(4)b	14.5	10844.813	10844.790	.023
P(1)a	7.5	10856.527	10856.430	.097
P(3)a	8.5	10863.882	10863.980	−.098
P(1)b	6.5	10870.406	10870.370	.036
R(4)b	13.5	10874.190	10874.200	−.010
P(3)a	7.5	10895.848	10895.910	−.062
R(4)b	12.5	10904.086	10903.970	(.116)
R(4)b	11.5	10923.657	10923.580	.077
P(3)b	6.5	10927.008	10927.170	(−.162)
R(1)b	19.5	10953.731	10953.710	.021
R(1)b	18.5	10974.810	10974.930	(−.120)
R(4)b	8.5	10978.881	10978.870	.011
R(4)b	7.5	10992.225	10992.210	.015
R(1)b	17.5	10993.492	10993.510	−.018
R(1)b	16.5	11003.879	11004.030	(−.151)
R(I)b	15.5	11015.399	11015.410	−.011
R(1)a	6.5	11015.485	11015.410	.075
R(1)a	17.5	11017.968	11018.060	−.092
R(1)b	7.5	11022.061	11021.960	(.101)
R(1)a	7.5	11022.735	11022.700	.035
R(1)b	10.5	11027.958	11028.020	−.062
R(1)a	8.5	11029.010	11028.970	.040
R(1)b	9.5	11030.120	11030.170	−.050
R(1)a	9.5	11033.316	11033.450	(−.134)
R(1)a	10.5	11037.162	11037.140	.022
R(1)b	11.5	11037.473	11037.540	−.067
R(1)a	11.5	11038.578	11038.500	.078
R(3)b	14.5	11038.969	11038.970	−.001
R(1)a	12.5	11039.589	11039.590	−.001
R(1)b	12.5	11043.411	11043.550	(−.139)
R(1)b	18.5	11044.120	11044.270	(−.150)
R(1)a	14.5	11044.595	11044.690	−.095